Identification of Catalytic Residues and Mechanistic Analysis of Family GH82 l-Carrageenases

ARTICLE *in* BIOCHEMISTRY · SEPTEMBER 2010

Impact Factor: 3.02 · DOI: 10.1021/bi1003475 · Source: PubMed

6 AUTHORS, INCLUDING:

Etienne Rebuffet
Institut Paoli Calmettes
16 PUBLICATIONS **216** CITATIONS
SEE PROFILE

Alexandra Jeudy
Pierre and Marie Curie University - Paris 6
8 PUBLICATIONS **121** CITATIONS
SEE PROFILE

Murielle Jam
Pierre and Marie Curie University - Paris 6
20 PUBLICATIONS **387** CITATIONS
SEE PROFILE

Gurvan Michel
French National Centre for Scientific Research
79 PUBLICATIONS **2,539** CITATIONS
SEE PROFILE

7590 *Biochemistry* **2010,** *49,* 7590–7599
DOI: 10.1021/bi1003475

BIOCHEMISTRY
including biophysical chemistry & molecular biology
Article

Identification of Catalytic Residues and Mechanistic Analysis of Family GH82 ι-Carrageenases[†]

Etienne Rebuffet, Tristan Barbeyron, Alexandra Jeudy, Murielle Jam, Mirjam Czjzek,* and Gurvan Michel

Université Pierre et Marie Curie and Centre National de la Recherche Scientifique, Marine Plants and Biomolecules UMR 7139, Station Biologique, 29682, Roscoff, France

Received March 7, 2010; Revised Manuscript Received August 3, 2010

ABSTRACT: Marine polysaccharide degrading enzymes, and ι-carrageenases in particular, have received little attention in the past, although their substrate specificity is of interest for biotechnological applications. This is mostly a consequence of the lack of data about their occurrence in the marine environment. Recent metagenomic data mining and the genome sequencing of a marine bacterium, *Zobellia galactanivorans*, led to the identification of three new ι-carrageenase genes belonging to the glycoside hydrolase family GH82. The additional sequences helped to identify potential candidate residues as catalytic proton donor and nucleophile. We have identified the catalytic key residues experimentally by site-directed mutagenesis and subsequent kinetic analysis for the ι-carrageenase from *Alteromonas fortis* CgiA1_Af. The kinetic analyses of the purified mutant enzymes confirm that E245 plays the role of the catalytic proton donor and D247 the general base that activates the catalytic water molecule. The point mutations of three other residues, namely, Q222, H281, and Q310 in *A. fortis*, located in proximity of the active site also affect the enzyme activity. Our results indicate that E310 plays a role in stabilizing the substrate intermediate conformation, while H281 is involved in substrate binding and appears to be crucial for maintaining the protonation state of the catalytic proton donor E245. The third residue, Q222, that bridges the catalytic water molecule and a chloride ion, plays a crucial role in structuring the water network in the active site of *A. fortis* ι-carrageenase.

The major matrix polysaccharides produced in the cell wall of carrageenophyte red algae (Rhodophyta) are sulfated galactans named carrageenans, which display key roles in important biologic processes, such as integrity of cell wall structure or signaling (*1*). They consist of a linear backbone of D-galactose residues linked by alternating α(1−3) and β(1−4) linkages. A further layer of complexity is the occurrence of a 3,6-anhydro bridge of the β(1−4)-linked galactose residue in κ- and ι-carrageenan and the number of ester-sulfate substituents per digalactose repeating unit, which varies from one in κ-carrageenan to two in ι-carrageenan and three in λ-carrageenan (*2*). Industrially extracted κ- and ι-carrageenans form thermoreversible gels in aqueous solution (*3*), a property that is exploited in many applications for food (*4*) or biomedical conditions (*5*).

In the ocean carrageenans represent an important carbon source for heterotrophic marine bacteria, which participate in this way in the recycling of red algal biomass (*6*). Bacteria are able to degrade fibers of carrageenans by enzymatic attack through glycoside hydrolases (GHs)[1] that are secreted into the external medium and/or attached to the bacterial cell wall. Interestingly, although the various carrageenans are chemically rather close, the respective GHs that degrade different types of carrageenans do not belong to the same family. Indeed, the κ-carrageenase is a member of family GH16 (*7*), the ι-carrageenase (iotase) belongs to family GH82 (*8*), while the λ-carrageenase is currently not classified (*9*).

While the first iotase activity has been described in 1984 by Greer et al (*10*), to date only two iotase sequences have been reported in literature, i.e., the first from the marine bacteria *Alteromonas fortis* and the second from *Zobellia galactanivorans* (*8*). While for the second enzyme only sequence data are available, the iotase of *A. fortis* has been studied more in detail, and the 3D crystal structure was solved in 2001 (*11*). The structure consists of a β-helix of ten complete turns, flanked by two domains (A and B) in the C-terminal region. The crystallographic structure of this enzyme was also solved in the presence of substrate oligocarrageenans, where a tetrasaccharide and a disaccharide have been located in subsites +4 to +1 and −3 to −4, respectively (*12*). Moreover, the complexed structure has highlighted that the catalytic cleft of the iotase adopts two conformations due to rigid body movement of the domain A: an open one, which allows for an initial endo attack of the carrageenan fibers, and a substrate-induced tunnel conformation, which accounts for the highly processive character of this enzyme (*12*). The *A. fortis* iotase hydrolyzes the β(1−4) bond by an inverting mechanism and produces neo-ι-carratetraose and neo-ι-carrahexaose as end products. It is generally accepted that inverting glycoside hydrolases catalyze the hydrolysis of the glycosidic bond via a single displacement reaction (*13*). One of the catalytic residues, acting as a general acid, provides protonic assistance to the departing glycosidic oxygen, whereas the second, acting as a general base,

[†]This work was supported by the French Region Bretagne and the Centre National de la Recherche Scientifique (CNRS). The fellowship of E.R. was jointly funded by Region Bretagne and CNRS (allocation number 211-B2-9/ARED).

*Corresponding author. Tel: +33 2 98 29 23 75. Fax: +33 2 98 29 23 24. E-mail: czjzek@sb-roscoff.fr.

[1]Abbreviations: GH, glycoside hydrolase; 3D, three dimensional; PCR, polymerase chain reaction; iotase or Cgi, ι-carrageenase; EDTA, ethylenedinitrilotetraacetic acid; HEPES, 4-(2-hydroxyethyl)piperazine-1-ethanesulfonic acid; SDS−PAGE, sodium dodecyl sulfate−polyacrylamide gel electrophoresis; C−PAGE, carbohydrate−polyacrylamide gel electrophoresis; PEG, polyethylene glycol; MME, monomethyl ester; MPD, methylpentanediol.

 Published on Web 08/03/2010

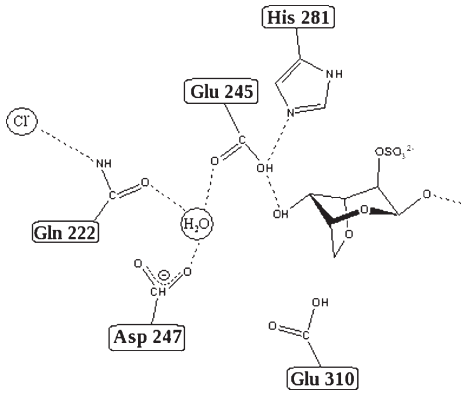

FIGURE 1: Schematic representation of the spatial arrangement of the residues located around the nonreducing end of the neocarratetraose unit bound to subsite +1 to +4 in the active site cleft of the ι-carrageenase, showing the relative position of the three potential catalytic residues, D247, E245, and E310, the catalytic water molecule, and the chloride ion.

activates a water molecule that effects a direct displacement at the anomeric center (*13*). However, the precise identity of these two catalytic residues for the enzymes belonging to family GH82 remains to be determined. The structural analysis has revealed that only three residues are strictly conserved in both sequences of *A. fortis* and *Z. galactanivorans* and located in the catalytic groove of the enzyme. For this reason it has been proposed that the catalytic residues are two among E245, D247, or E310 (*12*) (Figure 1).

Notably, recent genome sequencing projects, such as that of *Z. galactanivorans*, provide us with sequences of new members of family GH82 enzymes (Barbeyron et al., in preparation). Taking into account this new information and based on multiple sequence alignments of the various GH82 members, we have designed a site-directed mutagenesis study that, combined with the kinetic analysis, helps to define the roles of various residues that are key players in the catalytic mechanism of this enzyme family.

EXPERIMENTAL PROCEDURES

Molecular Biology and Enzymatic Assay of CgiA1_Zg, CgiA2_Zg, and CgiA3_Zg. The coding region of the mature iotases CgiA1_Zg, CgiA2_Zg, and CgiA3_Zg, i.e., without the N-terminal signal peptide, was amplified by the polymerase chain reaction (PCR) from the *Z. galactanivorans* DNA. The PCR products were inserted into pGEX and pET20b expression vectors, which were used to transform different expression strains of *Escherichia coli* (Origami (DE3) pLysS, BL21 (DE3), C41 (DE3), and C43 (DE3)). Expression was tested and observed only in *E. coli* Origami (DE3) pLysS for the CgiA1_Zg/pEt20b and CgiA3_Zg/pGEX constructions (data not shown). Recombinant *E. coli* cells were grown in ZYP medium (*14*) at 20 °C for 3 days. Then the cultures were centrifuged, and pellets were resuspended in 50 mM Tris, pH 8, 200 mM NaCl, 1 mM EDTA, and 10% glycerol buffer.

Since *E. coli* does not have any activity on ι-carrageenan, we could directly use the crude cell extract to test for the presence of enzyme activity within these two cell lines (Figure 2A). The cells were lysed with a French press, and the extract was centrifuged at 15000 rpm for 1 h. Twenty microliters of the supernatant was added to 80 μL of reagent solution to obtain a final composition of 0.3% ι/ν-carrageenan, 10 mM Tris, pH 8, and 200 mM NaCl. The substrate degradation was monitored by carbohydrate polyacrylamide gel electrophoresis (C−PAGE) using 6% (w/v) polyacrylamide for the stacking gel and 27% polyacrylamide for the running gel. The electrophoresis was performed at 200 V in 50 mM Tris-HCl and 1 mM EDTA buffer. The gel was stained in a 0.5% (w/v) Alcian blue solution for 10 min and subsequently with 0.4% (w/v) silver nitrate during 10 min. The detection was made with 1.75 g of Na_2CO_3, 20 μL of formaldehyde, and 25 mL of H_2OmQ.

Site-Directed Mutagenesis. The CgiA1_Af gene was mutagenized using the QuikChange site-directed mutagenesis kit (Stratagene). For each of the three potential catalytic residues, E245, D247, and E310, four amino acid residue replacements were chosen. In general, the amino acid E was changed to D (shortening of the side chain but maintaining the charge), A (elimination of side chain), N, or Q (elimination of charge). The amino acid D was changed to E, A, N, and Q with similar aims as mentioned above. All of these mutant clones were subsequently submitted to a medium-throughput heterologous expression strategy in *E. coli* (DE3) strains (see section Expression and Purification of CgiA1_Af and Mutants). The mutant clones that were successfully overexpressed in soluble form were then further scaled up to 1 L cultures to produce sufficient quantity for the enzymatic assays. Following this mutagenesis strategy, however, only one point mutant for each potential catalytic residue, namely, E245Q, D247A, and E310Q, was produced with reasonable yield. The point mutation for H281, replacing H by A, was chosen to eliminate the side chain. Several replacements for Q222 by E (introducing repulsive forces for the binding of a chloride ion), A (eliminating the side chain), K (to change the electrostatic nature of charge), and N (shortening of the side chain) were cloned and subsequently submitted to expression trials. In the end, however, only H281A, Q222E, and Q222K were overexpressed in soluble form.

Only the primers used to generate the successful mutations are indicated in Table 1. In all cases, we sequenced the resulting DNA to confirm that the mutations occurred at the correct, desired position.

Expression and Purification of CgiA1_Af and Mutants. Full details of the expression of wild-type *A. fortis* iotase have been described previously (*15*). Briefly, CgiA1_Af was expressed in M9 medium at 12 °C by the pET20b vector (Novagen) as a C-terminal His-tagged fusion protein in the periplasm of *E. coli* (DE3) strain. In the case of the recombinant mutant proteins, recombinant *E. coli* (DE3) cells were incubated at 288 K in ZYP medium. The culture was stopped when the cell growth reached the stationary phase. For both the wild-type and the mutant proteins, the cells were resuspended in a buffer composed of 50 mM HEPES, pH 7.5, 500 mM NaCl, and 100 mM imidazole (buffer A). The cells were lysed in a French press. After centrifugation at 15000 rpm for 2 h, the supernatant was loaded onto a 10 mL Chelating Fast Flow, $NiSO_4$-charged Sepharose column (GE Healthcare) and equilibrated with buffer A. The column was washed with buffer A and then eluted with 60 mL of a linear gradient of imidazole (100−500 mM). Fractions that showed the presence of iotase on sodium dodecyl sulfate−polyacrylamide gel electrophoresis (SDS−PAGE) were pooled and concentrated, and the buffer was exchanged against 50 mM HEPES, pH 7.5, and 100 mM NaCl buffer (buffer B). In a second step, the sample was loaded onto a 3 mL Source 15S (GE healthcare) column, previously equilibrated with buffer B. The column was washed with buffer B and then eluted with 30 mL of a linear gradient of

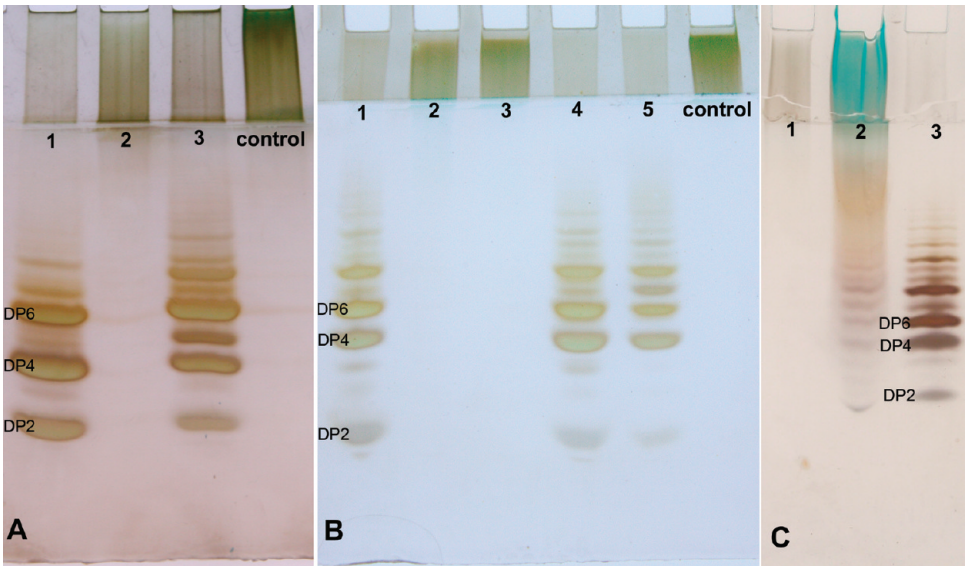

FIGURE 2: C−PAGE gels showing the degradation products of family GH82 iotases. In all cases 1 μg of enzyme was incubated with 100 μg of substrate at 0.3% for 6 h at 40 °C. One microliter of reaction mixture was deposited for all lanes. (A) Degradation products of crude extracts of *E. coli* strains expressing CgiA1_Zg (lane 1) and CgiA3_Zg genes (lane 3). (B) Degradation products of purified wild-type and mutant enzymes of CgiA1_Af. Lanes 1−5 show the wild type and mutants E245Q, D247A, E310Q, and H281A, respectively. (C) Degradation products of purified wild-type and mutant Q222E of CgiA1_Af under identical conditions as in (A) and (B). Deposition of 1 μL of reaction mixture (lane 1) and 20 μL (lane 2) containing mutant Q222E and 1 μL of reaction mixture with native enzyme (lane 3).

Table 1: Oligonucleotides Used To Mutagenize the ι-Carrageenase from *A. fortis*

mutant		primers $5' \rightarrow 3'$ [a]
E245Q	sense	GGAATTGCGTTACGGATG**CAG**ACTGACAACTTACTTATG
	antisense	TAAGTAAGTTGTCAGT**CTG**CATCCGTAACGCAATTCCGC
D247A	sense	GCGTTACGGATGGAAACT**GCG**AACTTACTTATG
	antisense	CATAAGTAAGTT**CGC**AGTTTCCATCCGTAACGC
E310Q	sense	GATAGTGGATTTGTC**CAG**CTCTTTAGCCCGACAG
	antisense	CTGTCGGGCTAAAGAG**CTG**GACAAATCCACTATC
H281A	sense	GCGGCGGTCATGTTTGGCCCA**GCT**TTTATGAAGAATGG
	antisense	CCATTCTTCATAAA**AGC**TGGGCCAAACATGACCGCCGC
Q222E	sense	GTTCGGCTACGGCCTTATT**GAA**ACCTATGGCGCAGATA
	antisense	TATCTGCGCCATAGGT**TTC**AATAAGGCCGTAGCCGAAC
Q222K	sense	GTTCGGCTACGGCCTTATT**AAA**ACCTATGGCGCAGATA
	antisense	TATCTGCGCCATAGGT**TTT**AATAAGGCCGTAGCCGAAC

[a] In each case, the mutated nucleotides are highlighted in bold.

NaCl (100−500 mM). The fractions that showed the presence of iotase on SDS−PAGE were pooled, concentrated, and dialyzed again 25 mM HEPES, pH 7.5, and 200 mM NaCl. All of mutant protein solutions were controlled by dynamic light scattering to be essentially monodisperse, using a Malvern Zetasizer to confirm that the mutants were properly folded. The values obtained for the respective hydrodynamic radius of gyration (R_h) are 7.6 ± 0.4 nm (wild type), 7.0 ± 0.3 nm (E245Q), 6.9 ± 0.5 nm (D247A), 6.8 ± 0.5 nm (E310Q), 7.4 ± 0.3 nm (H281A), 7.3 ± 0.4 nm (Q222K), and 7.6 ± 0.6 nm (Q222E) . The analyses of the final purified mutant enzymes on gels are shown in Figure 3. The concentrations of wild type, E245Q, D247A, E310Q, H281A, and Q222E were 0.45, 0.23, 0,58, 0.14, 1.0, and 0.22 mg/mL, respectively.

Enzyme Kinetics. Kinetic parameters for the hydrolysis of the hybrid polymer were determined spectrophotometrically using a stopped reducing sugar assay. Since no synthetic substrate analogues exist for this class of poly/oligosaccharides and to be able to perform the enzymatic kinetic measurements in solution, an ι-carrageenan composed of 80% of ι- and 20% of ν-carrageenan motif was used as substrate (*16*). This substrate is closer to the natural polysaccharide found in red algal cell walls, and the presence of ν-carrageenan blocks significantly decreases the

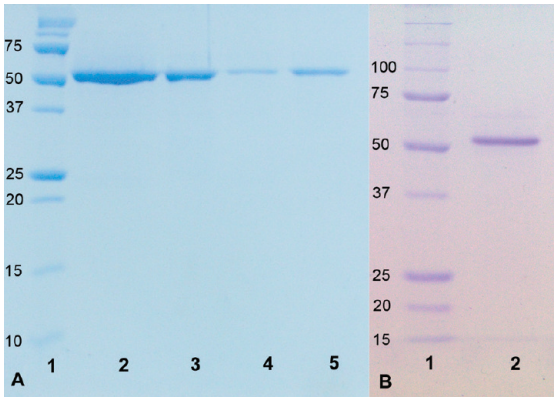

FIGURE 3: SDS−PAGE gel of purified wild-type and mutant enzymes. (A) Lanes 1−5 show the M_w markers, wild-type CgiA1_Af, and mutants E245Q, 247A, and E310Q, respectively. (B) Lane 1 shows M_w markers and lane 2 the purified mutant Q222K.

gelling properties of the polymer; hence it was possible to obtain solutions with relative high concentration.

Steady-state kinetic parameters were determined with a reaction mixture of 1 mL at 40 °C in 10 mM Tris, pH 8, and 100 mM NaCl that represent optimal salt and pH conditions for catalytic efficiency of the enzyme, as reported earlier (*10*). To further control the influence of chloride ions on enzymatic activity of wild-type iotase, attempts to measure enzymatic activity in the complete absence of chloride ions were performed by dialyzing the wild-type enzyme for 36 h against a solution containing 100 mM Tris at pH 7.5 adjusted by acetic acid instead of HCl. For these experiments the substrate was equally washed and dialyzed against 100 mM sodium acetate.

All experiments were performed in quadruplicate. The amount of released sugars was estimated by the ferricyanide reducing sugar assay (*17*). For all samples at least ten substrate concentrations in the range from 1.8% to 0.1% (w/v) were tested, and for each concentration at least eight time points were measured during a total reaction period of 20 min (wild type), 16 min (E310Q), and 90 min for the different samples, respectively. In all cases the reaction/ferricyanide mixture was maintained in boiling water during at least 10 min and cooled to room temperature before the absorbance was measured at 420 nm. A calibration curve with 50−300 μg/mL glucose was used to calculate the amount of reducing ends as glucose reducing end equivalents. The hyperbolic regression function of Hyper32, a hyperbolic regression program for the analysis of enzyme kinetic data (http://homepage.ntlworld.com/john.easterby/software.html), was used to determine the respective kinetic constants and statistics.

Oligosaccharide Production and Detection by C−PAGE. One hundred microliters of a 0.3% hybrid ι/ν-carrageenan solution with 10 mM Tris, pH 8, and 200 mM NaCl was incubated with 1 μg of enzyme at 40 °C for 6 h and subsequently boiled to stop the reaction. Substrate degradation of the different mutant enzymes are analyzed on C−PAGE gel as described for the *Z. galactanivorans* CgiA enzymes (Figure 2B,C).

Crystallization and Structure Refinement. Crystals of wild-type *A. fortis* iotase were grown at 19 °C in hanging drops composed of 1 μL of enzyme and 1 μL of reservoir solution containing 10% PEG 5000 MME, 100 mM sodium acetate, pH 5.5, 250 mM sodium nitrate, 2% MPD, and 0.02% ι-carrageenan. The crystals that appeared under these conditions were used for macroseeding in hanging drops composed of 1 μL of enzyme and 1 μL of reservoir containing 7% PEG 3350, 100 mM sodium acetate, pH 5.5, 250 mM sodium nitrate, and 10% glycerol. With the aim of structurally replacing the chloride ion in the crystals, they were soaked for 5 min in 10% PEG 3350, 100 mM sodium acetate, pH 5.5, and 250 mM sodium nitrate and containing 100 mM sodium bromide. Crystals were then quickly soaked in a crystallization solution supplemented with 30% glycerol and flash cooled at 100 K. Data were collected on a Bruker X8 proteum equipped with a PLATINUM 135 CCD detector. Data were integrated and scaled with the PROTEUM crystallographic software suite. The intensity data were converted to amplitudes using XPREP (as implemented in Bruker-AXS software (*18*)). The structure was determined by molecular replacement (PHASER) (*19*) using the coordinates of the native iotase (*11*) as a model, from which the A domain was deleted. Bragg diffraction was detectable to a maximum resolution of 2.48 Å; however, the data in the highest resolution shell shell was lacking completeness (51%) to be included in the structural refinement cycles. The data were therefore cut to have a nominal highest resolution of 2.6 Å being 72% complete. The initial molecular replacement solution was further refined with the program REFMAC5 (implemented within the CCP4 suite (*20*)), alternating with cycles of manual rebuilding in COOT (*21*). Data collection and refinement parameters are presented in Table 2. The refined coordinates and structure factors have been deposited at the Protein Data Bank with PDB accession code 3LMW.

Table 2: Data Collection and Refinement Statistics of the In-House Data Set of CgiA1_Af without Chloride

data collection	
wavelength (Å)	1.5418
space group	$P2_1$
unit cell parameters	
a, *b*, *c* (Å)	54.91, 101.19, 95.65
β (deg)	101.01
resolution range (Å)	68.83−2.6 (2.69−2.6)
no. of observations ($F > 0$)	239850 (7030)
no. of unique reflections	30829 (1953)
completeness (%)	95.1 (72.1)
mean $I/\sigma(I)$	14.3 (2.96)
R_{merge} (%)	6.3 (33.2)
redundancy	7.8 (3.6)
refinement	
resolution range	69.0−2.6
no. of unique reflections	28852
R factor (R_{free} on 5%)	18.4 (26.0)
no. of protein atoms (mean *B*-factor in Å^2)	7302 (20.2)
no. of solvent atoms (mean *B*-factor in Å^2)	332 (21.3)
no. of ions (mean *B*-factor in Å^2)	6 (36.0)
rmsd bond lengths (Å)	0.017
rmsd bond angles (deg)	1.55
mean overall *B*-factor (Å^2)	19.7
Ramachandran plot	
most favored region (%)	98.0
additionally allowed region (%)	1.8

Molecular Modeling. In a first step, domain A (residues 307−374) of the three ι-carrageenase structures, i.e., the native structure (id code 1H80), the closed conformation (id code 1KTW), and the one obtained in this study, was superimposed. The next step consisted in replacing the incomplete domain A of the complex structure by the complete one obtained in this study. This positioned the missing loop of domain A (residues 343−349) that covers the catalytic site in the closed conformation. Then the ι-carrageenan chain was completed, between the tetra- and the disaccharide units of the complex structure (1KTW), by adding the missing sugar units in the −2 and −1 binding sites such that a coherent octasaccharide with correct stereochemistry was obtained, spanning the entire binding site cleft. This procedure led to a structural model that reveals the close contacts between the iotase domain A with bound carrageenan units in the −1 and −2 subsites.

RESULTS

Sequence Alignment and Analysis of New Members of Family GH82 Enzymes. The recent success of marine genomic and metagenomic sequencing projects has provided us with new members of family GH82 enzymes. By regular BLAST searches against the newly deposited metagenomic flow of sequences, we have recently identified the sequence of a third, previously undescribed and incomplete ι-carrageenase in the meta-genome Sorcer II global ocean sampling (*22*). Moreover, our own project on the complete genome sequencing of the marine polysaccharide degrading flavobacterium *Z. galactanivorans* (Barbeyron et al., in

preparation) revealed the presence of two more sequences of family GH82 iotases in addition to the previously described and isolated one (*8*).

A multiple sequence alignment performed with Multalin (*23*) and Espript (*24*) of all currently available iotase genes and including the structural information from *A. fortis* is represented in Figure 4. The alignment reveals strong similarity in the core of the β-helix for CgiA1_Af, CgiA1_Zg, and CgiA1_Fi (called JCVI_PEP in the meta-genome database), which are particularly well conserved and besides having the same overall 3D fold also have the same domain architecture. Indeed, in these three sequences even the different domains are easily recognizable, since the β-helix core displays highest conservation, while the two insertion domains A and B in the C-terminal region of the enzyme (highlighted by red and green structural elements in Figure 4) are significantly less conserved. Interestingly, the two new sequences from *Z. galactanivorans* display sequence identity lower than 30% to the other three sequences. Moreover, they are significantly shorter with 429 and 329 amino acids for CgiA2_Zg and CgiA3_Zg, respectively, compared to CgiA1_Zg, which contains 491 residues. The difference in length is explained by the absence of domain A in CgiA2_Zg and the absence of both domains A and B in CgiA3_Zg.

Although the sequence alignment shows that most of the putative catalytic residues are indeed present in both CgiA2_Zg and CgiA3_Zg, the total absence of domains A and B raised the question whether these truncated variants of family GH82 ι-carrageenases still encode active enzymes. To answer this question, we have cloned the respective genes into *E. coli* expression strains to produce the recombinant proteins. After interaction with ι-carrageenan polymer, the analysis of the supernatant of the carrageenase-expressing *E. coli* strains (lane 3 in Figure 2A) clearly showed the production of oligosaccharides for CgiA1_Zg and CgiA3_Zg, demonstrating that the genes corresponding to these sequences indeed encode active ι-carrageenase enzymes.

Identification of the Catalytic Residues in the Sequence Alignment. The multiple sequence alignment shows that among the three expected catalytic residues, namely, E245, D247, and E310, only one, E245, is conserved in all five sequences. The analysis of the complexed crystal structure indicated that this residue is ideally positioned to be the proton donor and has been pointed out to be the most probable catalytic residue (*12*). Surprisingly, both of the other candidates are absent in at least one other sequence: D247 is not present in the sequence of CgiA2_Zg and E310 is absent in CgiA2_Zg and CgiA3_Zg. Two putative other candidates, close to E245, are highly conserved throughout the five sequences. This is the case of Q222, which is linked to a chloride ion through the side chain amine group, as revealed by the crystal structure. The second one is H281, which is involved in a hydrogen bond with E245 and, moreover, is in a particular ϵ-helix conformation in the crystal structure ("additionally allowed" region of the Ramachandran plot). These five positions were subsequently submitted to several residue replacements by site-directed mutagenesis using a parallel cloning strategy. For each critical position we were able to obtain one mutated enzyme overexpressed in soluble form, namely, Q222K, E245Q, D247A, H281A, and E310Q. The kinetic analyses of the point mutants of these highly conserved residues, located at the heart of the catalytic active site, are described in the following paragraph, identifying them as the key residues involved in the catalytic machinery in GH82 enzymes.

Kinetic Parameters of Point Mutants of Catalytic Candidate Residues in CgiA1_Af. In the laboratory, pure ι-carrageenan polymer is not a convenient substrate for kinetic studies of iotase, since it forms gels rapidly and at low concentrations. However, the hybrid ι/ν-carrageenan polymer (*16*), which in addition is closer to the natural substrate found in red algal cell walls, can be used as soluble substrate for kinetic measurements of the enzyme. Indeed, the ι-block structures, present in the polymer, are the substrate of the enzyme, while the ν-blocks decrease the gelling properties of the polymer by preventing the formation of ι-carrageenan double helix structure.

The kinetic parameters obtained with the wild type and various mutants of the *A. fortis* iotase are listed in Table 3. Our measurements of the kinetic parameters provide evidence that all five conserved residues do indeed have essential roles in catalysis. The K_m and k_{cat} values of the wild-type iotase are 8.5 mM and 726.6 s^{-1}, respectively. This results in an overall catalytic efficiency of 85.18 mM^{-1} s^{-1} for the wild-type CgiA1_Af iotase.

For two of the catalytic candidate mutants, E245Q and D247A, the enzymatic activity was completely abolished. No residual activity was measurable by the reducing sugar assay nor was the formation of oligosaccharides observed on the C−PAGE gel; all of the substrate was stained in the stacking gel. In agreement with their position revealed in the crystal structure (*11*), we experimentally confirm residues E245 and D247 (CgiA1_Af numbering) as the catalytic residues in GH82 iotase enzymes. Since no synthetic reagent to distinguish between the proton donor and the catalytic base of this inverting enzyme is actually available, as described for example by Shaikh et al. (*25*), this attribution is deduced from their position relative to the substrate in the crystal structure. Indeed, Michel et al. (*12*) had deduced that E245 is the catalytic proton donor, facilitating the cleavage of the glycosidic linkage via stabilization of the leaving group, and consequently D247 plays the role of the catalytic base, activating the hydrolytic water molecule in the single displacement reaction.

In the case of the mutant E310Q, the K_m value is reduced by a factor of about 4, indicating that apparently the enzyme binds better to the substrate. But the reduction in k_{cat} by 50-fold resulted in a substantial decrease in the overall enzyme efficiency (about 10-fold). We conclude that E310 is not a residue directly involved in catalysis, but the 10-fold decrease of efficiency indicates that it does participate indirectly in the catalytic reaction.

The mutant enzyme H281A also decreases the K_m in a similar manner as E310Q by 7-fold, but the decrease in k_{cat} by 180-fold is even more pronounced. Consequently, the enzyme efficiency is also strongly affected by this mutation. Indeed, H281 is involved in a tight hydrogen bond with the proton donor E245: $N^{\epsilon 2}$ of the histidine side chain forms a hydrogen bond (2.57 Å) to one carboxyl oxygen ($O^{\epsilon 2}$) of E245.

Two mutations of Q222 were successfully expressed in *E. coli* strains, namely, Q222K and Q222E. However, for both mutated enzymes no kinetic measurements were possible. The *E. coli* strain expressing the Q222E-iotase did show activity when growing on ι-carrageenan gel containing plates, and we expressed and purified this mutant in quantities suitable for kinetic analysis. However, the activity was not pronounced enough to perform a complete enzymatic assay. Analysis by C−PAGE of the reaction products, under same conditions as for the native enzyme, revealed a very low production of oligosaccharides, and 20 times more reaction mixture needs to be deposited to reveal some

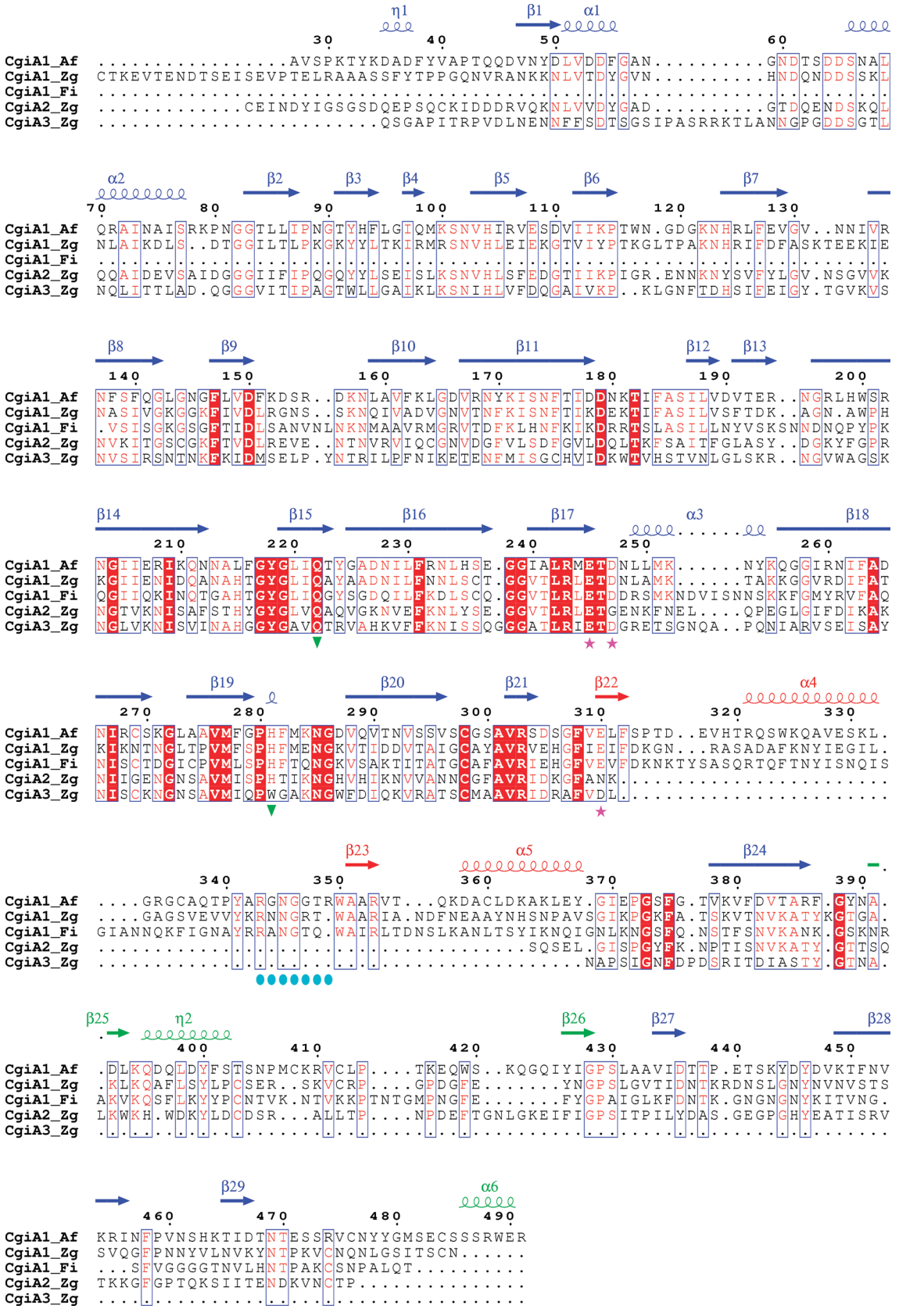

FIGURE 4: Multiple sequence alignment of all five members of GH82 iotase enzymes. The secondary structure elements above the sequences correspond to those observed in the crystal structure of CgiA1_Af. The different domains are colored in blue (β-helix core structure), red (domain A), and green (domain B), respectively. Pink stars below the sequences indicate the catalytic proton donor (E245), the general base (D247), and E310, the light blue circles below the sequences mark the disordered loop of domain A, while the green triangles mark Q222 and H281. CgiA1_Fi designates the combined sequence of two peptides JCVI_gs031_1105100132297 and JCVI_gs031_1105100129569 that have been identified in the global ocean meta-genome data set (*22*).

residual activity (Figure 2C). The mutant Q222K-iotase was also expressed soluble in sufficient amounts to perform the complete purification steps (Figure 3B), indicating that the protein is correctly folded (also confirmed by a relative monodisperse peak

Table 3: Steady-State Kinetic Parameters for Hydrolysis of Hybrid Carrageenan by Recombinant Wild-Type and Mutant ι-Carrageenase from *A. fortis*[a]

enzyme	K_m (mM)	k_{cat} (s^{-1})	k_{cat}/K_m (mM^{-1} s^{-1})	relative efficiency (%)
wild type	8.5 ± 3.7	726.6 ± 94.0	85.18	100
E245Q	ND[b]	ND	ND	ND
D247A	ND	ND	ND	ND
E310Q	2.4 ± 0.4	13.8 ± 0.7	5.75	7
H281A	1.2 ± 0.4	4.1 ± 0.2	3.42	4
Q222E	ND	ND	ND	ND
Q222K	ND	ND	ND	ND

[a]The experiments were carried out at least at ten different substrate concentrations, and the parameters were calculated using Hyper32. [b]ND, no hydrolysis detectable.

in dynamic light scattering measurements), but this mutant was inactive in all tests, and no oligosaccharides are revealed on a C−PAGE gel (not shown).

Description of the Iotase Structure in the Novel Crystal Form. The crystal structure of CgiA1_Af in a new crystal form, in the presence of sodium bromide, belonged to space group $P2_1$ and was determined to a resolution of 2.6 Å (unit cell parameters in Table 2). Two enzyme molecules are found per asymmetric unit, leading to a V_M of 2.34 $Å^3$/Da and a solvent content of 47.5%. The refinement of 7302 protein atoms that cover residues 28−499, including residues 343−349 (only for molecule A) that were disordered in the previous structures, 6 ions (Ca^{2+}, Ni^{2+}, and NO_3^-), and 332 water molecules led to an overall *R* factor of 18.4% and a R_{free} factor of 26.0%. Furthermore, the close inspection of the chloride position, observed previously in the iotase crystal structures (*11*), revealed that in the crystal form obtained here this position was empty in molecule A and displayed weak electron density in molecule B. Moreover, the conserved water network filling the active site cleft was affected, and many water molecules appeared to be excluded by the absence of the negative charge at the chloride ion position. Given the medium resolution of the crystal structure at 2.6 Å, however, we cannot exclude the possibility that data incompleteness and limited resolution are the explanation for the lack of electron density for water molecules in the active site groove.

As expected, the overall crystal structure (Figure 5A) is highly similar to those already described in the native and complexed form by Michel et al (*11*, *12*); however, domain A clearly takes a different position from the two described earlier (Figure 5B). In molecule A this domain is stabilized through crystal packing contacts in a position even more open than in the other two structures (Figure 5B). As a consequence all residues of domain A are ordered in molecule A, and the construction of the complete domain A, including the missing loop from residues 343 to 349, was possible.

Having access to various structural conformations as well as a partial substrate complex of the iotase, we have modeled, by subsequent superimposition and replacement, the closed domain A conformation onto the substrate complex, in which we have connected the two product molecules, present in 1KTW, by a neo-ι-carrabiose to obtain a continuous ι-carrageenan chain spanning the active site cleft. Possible protein−substrate interactions could be inferred from this model. Indeed, two arginine residues (R343 and R349) present in the disordered part of the loop are in close contact with the sulfate-ester groups of the neo-ι-carrabiose units bound in subsites −1 and −2 (Figure 6).

DISCUSSION

We have performed a site-directed mutagenesis study in combination with a crystal structure and activity measurements of the enzyme in the absence of chloride ions to experimentally probe the role of specific residues and the chloride ion in the catalytic mechanism of a family GH82 ι-carrageenase. The complete inactivity of soluble expressed mutants E245Q and D247A, together with the relative position of these residues in the crystal structure, confirms E245 to be the proton donor and D247 the general base that activates the catalytic water molecule. Since these residues are critical to the mechanism, their removal has a significant effect on catalysis, as expected for inverting enzymes (*26*). Interestingly, D247 is not present in the sequence of CgiA2_Zg, where it is replaced by a glycine. Generally, it is rather rare that one of the two crucial catalytic carboxylic acids is absent in active glycoside hydrolases. But in some cases such replacements do take place. For example, in family GH1 myrosinases, the catalytic proton donor is replaced by a glutamine residue, and the leaving group activation is assisted by an ascorbate cofactor (*27*). Another interesting recent example, where the catalytic machinery is not conserved within a family, is the GH97 enzymes, but in this case the change of position of the general base transforms an inverting enzyme into a retaining one (*28*). Noteworthy, a third type of enzymes, where the exact position of the catalytic machinery is not strictly conserved, can be found in retaining enzymes of family GH16. Indeed, the catalytic residues are carried by a conserved motif EID[I,V](X)E, where in some members (β-agarases, κ-carrageenases) the motif contains a β-bulge, whereas other members (XET and lichenases) display a regular β-strand (*29*).

The fact that the mutation of H281 strongly affects the catalytic efficiency clearly indicates that this residue is also important for the catalytic cycle. Such hydrogen bonds, formed by a histidine residue with the catalytic residues, have also been observed in family GH16 and GH7 glycoside hydrolases (*29*, *30*). The histidine is thought to be involved in proton trafficking, thus ensuring regeneration of the correct protonated states of the catalytic residues throughout the enzymatic pathway.

The first crystal structure of the iotase from *A. fortis* has revealed the presence of a chloride ion in the proximity of the catalytic active site (*11*). The chloride ion is bound to Q222 that in turn is hydrogen bonding the catalytic water molecule. Our results show that mutation of Q222 into a lysine leads to an inactive enzyme, while in the case of replacement with a glutamic acid, although very low, activity still is present (Figure 2C). This behavior might well be explained by electrostatic effects, needed to activate (polarize) the nucleophilic water molecule, indirectly involving both Q222 and the chloride ion in the catalytic cycle; their role might be the activation and replacement and/or turnover of the water molecule that is hydrolyzing the glycosidic bond. The lysine replacing the glutamine residue would still bind the chloride ion but cannot establish a further hydrogen bond activating or positioning the catalytic water molecule. A glutamic acid at this position, due to its charged character, possibly impairs the binding of a chloride ion, leading to a more instable enzyme, but the charged side chain may still activate the catalytic water molecule, explaining the residual activity observed on C−PAGE gels.

Interestingly, residues with hydroxyl groups, that might be equivalents of the chloride/glutamine pair in CgiA1_Af, were found in the close environment of the general base in several

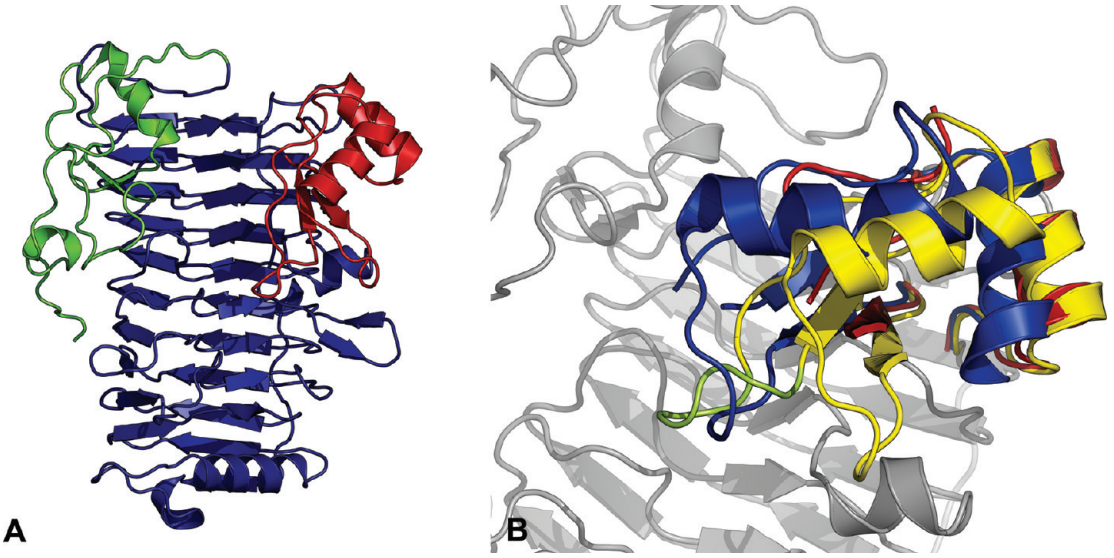

FIGURE 5: Crystal structure of CgiA1_Af in the absence of chloride ions. (A) Ribbon representation of the β-helical structure is in blue; domains A and B are colored in red and green, respectively. (B) Superimposition of the different structures of CgiA1_Af highlighting the mobility of domain A: red, first crystal structure (1H80); blue, crystal structure of CgiA1_Af in complex with oligo-ι-carrageenan (1KTW); yellow, molecule A of this crystal structure in the absence of chloride ions.

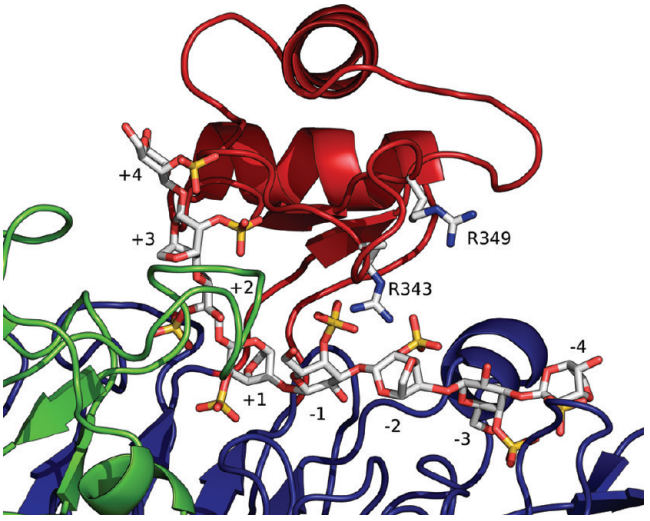

FIGURE 6: Ribbon representation of the model obtained of CgiA1_Af showing the complete domain A in the presence of an ι-carrageenan chain spanning the entire active site cleft. Two well-conserved arginine residues of domain A (R343 and R349) that are in positions to interact with the substrate molecule are highlighted.

other inverting glycoside hydrolases. Their respective roles are to orientate the catalytic water molecule in a position for optimal catalysis. This is the case of Thr45 in chitosanase (GH46) from *Streptomyces* sp. (*31*), Tyr203 in xylanase (GH8) from *Pseudoalteromonas haloplanktis* (*32*), Ser190 in chitinase (GH19) ChiC from *Pseudomyces griseus* (*33*), and Ser120 in chitinase (GH19) in barley seeds (*34*). In CgiA1_Af, the side chain of Q222 together with the more distant chloride ion may well influence the exact positioning of the catalytic water and the complete water network, necessary to provide the reaction with a new hydrolytic agent. Interestingly, this residue is strictly conserved in all known iotase sequences (Figure 4), indicative of a relatively important role of this residue. Moreover, Greer and Yaphe (*10*) have shown that the activity of the enzyme is dependent on NaCl. Optimal ι-carrageenase activity is obtained when the concentration of NaCl is between 100 and 500 mM. Moreover, our attempts to measure enzymatic activity in the absence of chloride ions, by extensive dialysis of the iotase and the substrate prior to the activity tests, generally showed a substantial decrease in activity by at least 60% (data not shown). However, the reproducibility of these trials was not consistent, most probably due to difficulties in producing completely chloride-free enzyme and substrate solutions. Interestingly, when soaking the crystals of CgiA1_Af in 100 mM sodium bromide containing solution, the subsequent crystal structure showed the absence of any ion at the corresponding position. Our chloride-free conditions allowed removing the chloride ion, but the bromide ion could not replace it. Apparently, the ion binding pocket is highly specific for chloride. Discrimination might be obtained by the van der Waals radius of the ions, explaining that the larger bromide does not replace a chloride ion. A remarkable consequence of the unoccupied chloride pocket is the disappearance of the conserved water network, including the catalytic water molecule, in the close vicinity of the active site (Figure 7). The absence of electron density that can be modeled as water molecules does not mean that no water molecules are present but most probably that the water molecules are much more labile and have undefined positions. Consequently, the catalytic water orientation is not optimal and the enzyme less efficient. However, having determined this crystal structure at medium resolution of 2.6 Å, we cannot exclude the possibility that phase truncation errors are the reason for the missing water molecules in this structural model.

A somewhat similar role of a chloride ion, although much more direct, has been observed in the active site of some GH13 α-amylases. In these enzymes the chloride ion is directly involved in polarizing the hydrolytic water molecule and enhances the rate of the second step in the catalytic reaction (*35*−*37*).

The decrease of catalytic efficiency, provoked by the E310Q mutation, may be explained by a role of this residue in stabilizing tyrosine 341. In both the native and complexed structures (refs *11* and *12* and this study), Glu310 is involved (through the carboxylic group) in a hydrogen bond with the hydroxyl group of Y341. The side chain of this latter residue therefore has no conformational freedom. Changing Glu310 into a glutamine removes this hydrogen bond, and the side chain of Y341 may be

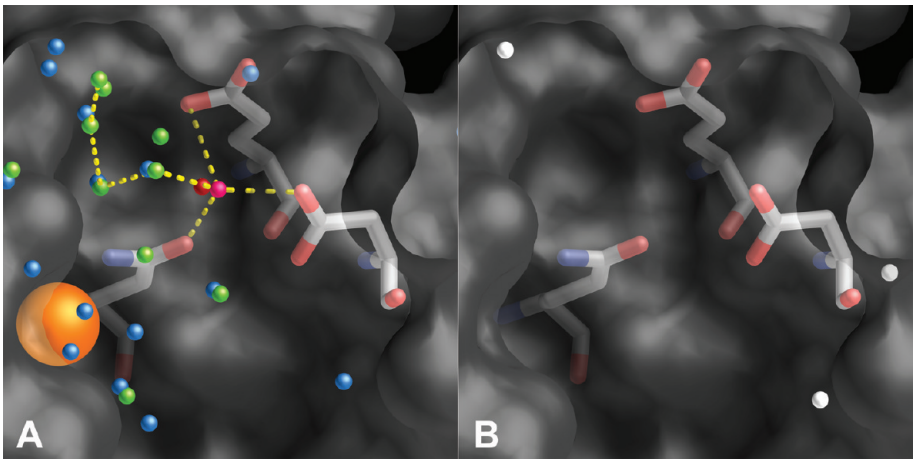

FIGURE 7: (A) Surface representation of CgiA1_Af (1H80—blue and red balls and 1KTW—green and pink balls) showing the network of conserved water molecules that fill the active site cleft (*11*). (B) Surface representation of CgiA1_Af in the absence of chloride ions (this study) showing that most of the conserved waters are disordered or excluded at the active site.

more flexible and therefore adapts better with the substrate in subsite +2. Through the higher flexibility, Y341 might bind tighter to the substrate, which would explain the decrease of the K_m value. In contrast, the decrease of k_{cat} would be the consequence of a bad positioning of the glycosidic bond and/or a diminished ability of the enzyme to slide along the ι-carrageenan chain.

Another interesting feature encountered in the two new ι-carrageenase sequences in *Z. galactanivorans* is the absence of domain A in both enzymes (Figure 4). Michel et al. (*12*) have shown that domain A is involved in the formation of a tunnel, a movement and character that most probably confer the processive mode of action to the enzyme. The absence of this domain in CgiA2 and CgiA3 (and consequently the absence of Q310 and Y341 discussed above) therefore may confer a different mode of action to these enzymes. In addition, the complete domain A in our molecular model, including the disordered loop containing several arginine residues, is positioned such that R343 and R349 are in close contact to the neo-ι-carrabiose units that bind to subsites −1 and −2 (Figure 6). Interestingly, R343 is conserved in all three iotase-like genes that contain domain A. In contrast to chitinases or cellulases, where the sliding along the substrate is mostly aided by aromatic residues (*36*), the mechanism of processivity in ι-carrageenases could also involve arginine residues that "pull" along the negative charges of the sulfate-ester groups. Thus, taking together all the missing factors, we believe that the iotases of the type of CgiA2 and CgiA3 might display a mode of action other than processive. Furthermore, in the case of CgiA3-type enzymes the absence of domain B (involved in substrate recognition and binding at subsites +1, +2, and +3) might lower the stretch of ι-carrageenan blocks necessary for the enzyme to be active, by reducing the numbers of subsites from 8 to 6 or less. Consequently, and in analogy to other complex polysaccharide degrading systems (*38*), we expect the three paralogous enzymes present in *Z. galactanivorans* to work in synergy to efficiently degrade ι-carrageenan in its solid state. A highly efficient degradation system would represent a net advantage for the bacteria when associated to carrageenophyte algae. However at this stage, the case of *Z. galactanivorans* having three paralogous GH82 enzymes still is unique.

The sequence of the iotase-like gene CgiA1_Fi, identified in a metagenome data set taken in the ocean close to Fernandina Island (*22*), is not complete, but from the part of the identified sequence that is present, we can deduce that the enzyme is of type CgiA1. Overall, resulting from our data mining analysis, this type of iotase appears therefore to be the most common form. The complete genome sequencing of several more marine bacteria will be necessary to conclude on the frequency and occurrence of this type of enzymes in the marine environment. Furthermore, the production of recombinant protein of CgiA2 and CgiA3 from *Z. galacanivorans* in sufficient quantity and quality to perform further enzymatic and structural studies will provide us with more information about the variation of mode of action within GH82 enzymes. This work is currently ongoing.

ACKNOWLEDGMENT

We thank W. Helbert and the group "structure of marine polysaccharides" for helpful discussions and for providing the hybrid ι/ν-carrageenan polysaccharide sample.

REFERENCES

1. Potin, P., Bouarab, K., Kupper, F., and Kloareg, B. (1999) Oligosaccharide recognition signals and defence reactions in marine plant-microbe interactions. *Curr. Opin. Microbiol. 2*, 276–283.
2. Kloareg, B., and Quatrano, R. (1988) Structure of the cell walls of marine algae and ecophysiological functions of the matrix polysaccharides. *Oceanogr. Mar. Biol. Ann. Rev. 26*, 259–315.
3. Rees, D. (1969) Structure, conformation, and mechanism in the formation of polysaccharide gels and networks. *Adv. Carbohydr. Chem. Biochem. 24*, 267–332.
4. de Ruiter, G., and Rudolph, B. (1997) Carrageenan biotechnology. *Trends Food Sci. Technol. 8*, 389–395.
5. Carlucci, M., Pujol, C., Ciancia, M., Noseda, M., Matulewicz, M., Damonte, E., and Cerezo, A. (1997) Antiherpetic and anticoagulant properties of carrageenans from the red seaweed *Gigartina skottsbergii* and their cyclized derivatives: correlation between structure and biological activity. *Int. J. Biol. Macromol. 20*, 97–105.
6. Michel, G., Nyval-Collen, P., Barbeyron, T., Czjzek, M., and Helbert, W. (2006) Bioconversion of red seaweed galactans: a focus on bacterial agarases and carrageenases. *Appl. Microbiol. Biotechnol. 71*, 23–33.
7. Barbeyron, T., Henrissat, B., and Kloareg, B. (1994) The gene encoding the κ-carrageenase of *Alteromonas carrageenovora* is related to beta-1,3-1,4-glucanases. *Gene 139*, 105–109.
8. Barbeyron, T., Michel, G., Potin, P., Henrissat, B., and Kloareg, B. (2000) ι-Carrageenases constitute a novel family of glycoside hydrolases, unrelated to that of κ-carrageenases. *J. Biol. Chem. 275*, 35499–35505.
9. Guibet, M., Colin, S., Barbeyron, T., Genicot, S., Kloareg, B., Michel, G., and Helbert, W. (2007) Degradation of λ-carrageenan by *Pseudoalteromonas carrageenovora* λ-carrageenase: a new family of glycoside hydrolases unrelated to kappa- and ι-carrageenases. *Biochem. J. 404*, 105–114.

10. Greer, C. W., and Yaphe, W. (1984) Purification and properties of ι-carrageenase from a marine bacterium. *Can. J. Microbiol. 30*, 1500–1506.
11. Michel, G., Chantalat, L., Fanchon, E., Henrissat, B., Kloareg, B., and Dideberg, O. (2001) The ι-carrageenase of *Alteromonas fortis*. A beta-helix fold-containing enzyme for the degradation of a highly polyanionic polysaccharide. *J. Biol. Chem. 276*, 40202–40209.
12. Michel, G., Helbert, W., Kahn, R., Dideberg, O., and Kloareg, B. (2003) The structural bases of the processive degradation of ι-carrageenan, a main cell wall polysaccharide of red algae. *J. Mol. Biol. 334*, 421–433.
13. Sinnott, M. L. (1990) Catalytic mechanisms of glycosyl transfer. *Chem. Rev. 90*, 1171–1202.
14. Studier, F. W. (2005) Protein production by auto-induction in high density shaking cultures. *Protein Expression Purif. 41*, 207–234.
15. Michel, G., Flament, D., Barbeyron, T., Vernet, T., Kloareg, B., and Dideberg, O. (2000) Expression, purification, crystallization and preliminary X-ray analysis of the ι-carrageenase from *Alteromonas fortis*. *Acta Crystallogr., Sect. D: Biol. Crystallogr. 56*, 766–768.
16. Guibet, M., Boulenguer, P., Mazoyer, J., Kervarec, N., Antonopoulos, A., Lafosse, M., and Helbert, W. (2008) Composition and distribution of carrabiose moieties in hybrid κ/ι-carrageenans using carrageenases. *Biomacromolecules 9*, 408–415.
17. Kidby, D. K., and Davidson, D. J. (1973) A convenient ferricyanide estimation of reducing sugars in the nanomole range. *Anal. Biochem. 55*, 321–325.
18. Sheldrick, G. M. (2008) A short history of SHELX. *Acta Crystallogr. A 64*, 112–122.
19. McCoy, A. J., Grosse-Kunstleve, R. W., Adams, P. D., Winn, M. D., Storoni, L. C., and Read, R. J. (2007) Phaser crystallographic software. *J. Appl. Crystallogr. 40*, 658–674.
20. Collaborative Computational Project Number 4 (1994) The CCP4 suite: programs for protein crystallography. *Acta Crystallogr., Sect. D: Biol. Crystallogr. 50*, 760–763.
21. Emsley, P., and Cowtan, K. (2004) Coot: model-building tools for molecular graphics. *Acta Crystallogr., Sect. D: Biol. Crystallogr. 60*, 2126–2132.
22. Rusch, D. B., Halpern, A. L., Sutton, G., Heidelberg, K. B., Williamson, S., Yooseph, S., Wu, D., Eisen, J. A., Hoffman, J. M., Remington, K., Beeson, K., Tran, B., Smith, H., Baden-Tillson, H., Stewart, C., Thorpe, J., Freeman, J., Andrews-Pfannkoch, C., Venter, J. E., Li, K., Kravitz, S., Heidelberg, J. F., Utterback, T., Rogers, Y. H., Falcon, L. I., Souza, V., Bonilla-Rosso, G., Eguiarte, L. E., Karl, D. M., Sathyendranath, S., Platt, T., Bermingham, E., Gallardo, V., Tamayo-Castillo, G., Ferrari, M. R., Strausberg, R. L., Nealson, K., Friedman, R., Frazier, M., and Venter, J. C. (2007) The Sorcerer II Global Ocean Sampling expedition: northwest Atlantic through eastern tropical Pacific. *PLoS Biol 5*, e77.
23. Corpet, F. (1988) Multiple sequence alignment with hierarchical clustering. *Nucleic Acids Res. 16*, 10881–10890.
24. Gouet, P., Robert, X., and Courcelle, E. (2003) ESPript/ENDscript: Extracting and rendering sequence and 3D information from atomic structures of proteins. *Nucleic Acids Res. 31*, 3320–3323.
25. Shaikh, F. A., Randriantsoa, M., and Withers, S. G. (2009) Mechanistic analysis of the blood group antigen-cleaving endo-β-galactosidase from *Clostridium perfringens*. *Biochemistry 48*, 8396–8404.
26. Damude, H. G., Withers, S. G., Kilburn, D. G., Miller, R. C. J., and Warren, R. A. (1995) Site-directed mutation of the putative catalytic residues of endoglucanase CenA from *Cellulomonas fimi*. *Biochemistry 34*, 2220–2224.
27. Burmeister, W. P., Cottaz, S., Rollin, P., Vasella, A., and Henrissat, B. J. B. C. (2000) High resolution X-ray crystallography shows that ascorbate is a cofactor for myrosinase and substitutes for the function of the catalytic base. *J. Biol. Chem. 275*, 39385–39393.
28. Gloster, T. M., Turkenburg, J. P., Potts, J. R., Henrissat, B., and Davies, G. J. (2008) Divergence of catalytic mechanism within a glycosidase family provides insight into evolution of carbohydrate metabolism by human gut flora. *Chem. Biol. 15*, 1058–1067.
29. Michel, G., Chantalat, L., Duee, E., Barbeyron, T., Henrissat, B., Kloareg, B., and Dideberg, O. (2001) The κ-carrageenase of *P. carrageenovora* features a tunnel-shaped active site: a novel insight in the evolution of Clan-B glycoside hydrolases. *Structure 9*, 513–525.
30. Kleywegt, G. J., Zou, J. Y., Divne, C., Davies, G. J., Sinning, I., Stahlberg, J., Reinikainen, T., Srisodsuk, M., Teeri, T. T., and Jones, T. A. (1997) The crystal structure of the catalytic core domain of endoglucanase I from *Trichoderma reesei* at 3.6 Å resolution, and a comparison with related enzymes. *J. Mol. Biol. 272*, 383–397.
31. Lacombe-Harvey, M. E., Fukamizo, T., Gagnon, J., Ghinet, M. G., Dennhart, N., Letzel, T., and Brzezinski, R. (2009) Accessory active site residues of *Streptomyces* sp. N174 chitosanase: variations on a common theme in the lysozyme superfamily. *FEBS J. 276*, 857–869.
32. Collins, T., De Vos, D., Hoyoux, A., Savvides, S. N., Gerday, C., Van Beeumen, J., and Feller, G. (2005) Study of the active site residues of a glycoside hydrolase family 8 xylanase. *J. Mol. Biol. 354*, 425–435.
33. Kezuka, Y., Ohishi, M., Itoh, Y., Watanabe, J., Mitsutomi, M., Watanabe, T., and Nonaka, T. (2006) Structural studies of a two-domain Chitinase from *Streptomyces griseus* HUT6037. *J. Mol. Biol. 358*, 472–484.
34. Hart, P. J., Pfluger, H. D., Monzingo, A. F., Hollis, T., and Robertus, J. D. (1995) The refined crystal structure of an endochitinase from *Hordeum vulgare* L. seeds at 1.8 Å resolution. *J. Mol. Biol. 248*, 402–413.
35. Aghajari, N., Feller, G., Gerday, C., and Haser, R. (2002) Structural basis of alpha-amylase activation by chloride. *Protein Sci. 11*, 1435–1441.
36. Feller, G., Narinx, E., Arpigny, J. L., Aittaleb, M., Baise, E., Genicot, S., and Gerday, C. (1996) Enzymes from psychrophilic organisms. *FEMS Microbiol. Rev. 18*, 189–202.
37. Numao, S., Maurus, R., Sidhu, G., Wang, Y., Overall, C. M., Brayer, G. D., and Withers, S. G. (2002) Probing the role of the chloride ion in the mechanism of human pancreatic alpha-amylase. *Biochemistry 41*, 215–225.
38. Teeri, T. T. (1997) Crystalline cellulose degradation: new insight into the function of cellobiohydrolases. *Trends Biotechnol. 15*, 160–167.